EEG-Based Classification of Fast and Slow Hand Movements Using Wavelet-CSP Algorithm

Neethu Robinson*, A. P. Vinod, *Senior Member, IEEE*, Kai Keng Ang, Keng Peng Tee, and Cuntai T. Guan, *Senior Member, IEEE*

***Abstract*—A brain–computer interface (BCI) acquires brain signals, extracts informative features, and translates these features to commands to control an external device. This paper investigates the application of a noninvasive electroencephalography (EEG)-based BCI to identify brain signal features in regard to actual hand movement speed. This provides a more refined control for a BCI system in terms of movement parameters. An experiment was performed to collect EEG data from subjects while they performed right-hand movement at two different speeds, namely fast and slow, in four different directions. The informative features from the data were obtained using the Wavelet-Common Spatial Pattern (W-CSP) algorithm that provided high-temporal-spatial-spectral resolution. The applicability of these features to classify the two speeds and to reconstruct the speed profile was studied. The results for classifying speed across seven subjects yielded a mean accuracy of 83.71% using a Fisher Linear Discriminant (FLD) classifier. The speed components were reconstructed using multiple linear regression and significant correlation of 0.52 (Pearson's linear correlation coefficient) was obtained between recorded and reconstructed velocities on an average. The spatial patterns of the W-CSP features obtained showed activations in parietal and motor areas of the brain. The results achieved promises to provide a more refined control in BCI by including control of movement speed.**

***Index Terms*—Brain–computer interfaces (BCIs), common spatial patterns (CSPs), discrete wavelet transform (DWT), electroencephalography (EEG), movement-related parameters, multiple linear regression.**

I. Introduction

THE brain–computer interface (BCI) provides an additional output channel from brain, and uses the neuronal activity of brain to control effectors such as robotic arm or wheel chair; or to restore motor abilities of paralyzed or stroke patients [1], [2]. The core components of a BCI system [2], [3] are brain signal acquisition, preprocessing, feature extraction, classification, translation, and feedback control of external devices. Based on the type of sensors used for the data acquisition, BCI systems can be invasive or noninvasive.

Electroencephalography (EEG) [4] is a widely used noninvasive BCI due to its low expense and high-temporal resolution. The EEG data acquisition is followed by a preprocessing stage, which attenuates the artifacts and noises present in the brain signal, to enhance the relevant information. The subsequent feature extraction stage is responsible for forming discriminative set of features in the form of frequency patterns [5], temporal patterns [6], time-frequency patterns [7], autoregressive models [8], or spatial patterns [9], [10] for each task performed. The features extracted are used to train a classifier to decode the users' intent and subsequently translate the features into a set of output commands for operating an external device. The challenges in developing an efficient feature extraction and machine learning technique in an EEG-based BCI are the high temporal-spectral and spatial resolution, high robustness, and online adaptation capability to compensate for nonstationarity [1]. Hence, advanced signal processing, pattern recognition techniques, and efficient classifiers play a key role in this field of neuroscience research.

One of the major applications of BCI is in the rehabilitation of patients with neuromuscular disorders, who are incapable of limb movement. However, the limited number of control commands available is currently a much addressed issue in this area of EEG-based BCI research. Most of the BCIs that studied movement-related features use brain signals during movement of different body parts such as right hand, left hand, foot, and tongue [11]. The identification of brain signal components responsible for movement parameters such as speed, direction or extent of hand movement is a challenging area of research. It has been assumed that the movement-related parameters are encoded in the neuronal firing of motor cortex but cannot be decoded by noninvasive signal recordings [12], [14]. Recently several studies [15]–[22] showed the presence of sufficient information in surface Magnetoencephalography (MEG) and EEG to yield information regarding movement kinematics. The study in [16] reported the presence of movement information in the very low-frequency (LF) bands of the EEG data. It also reported that despite the strong movement-related power suppressions observed in the beta band (13–30 Hz) and power increase in the gamma band (>30 Hz), signals in these frequency ranges were less efficient than the LF band (<5 Hz) for movement parameter decoding. Electrocorticography (ECoG) was used in [13] to analyze differential representation of an arm movement and the authors showed that the spectral amplitude modulation in

Manuscript received August 13, 2012; revised December 14, 2012 and February 14, 2013; accepted February 14, 2013. Date of publication February 21, 2013; date of current version July 13, 2013. This work was supported by the Nanyang Technological University, Singapore. *Asterisk indicates corresponding author.*

*N. Robinson is with the Nanyang Technological University, Singapore 639798 (e-mail: neethu1@e.ntu.edu.sg).

A. P. Vinod is with the Nanyang Technological University, Singapore 639798 (e-mail: asvinod@ntu.edu.sg).

C. T. Guan, K. K. Ang, and K. P. Tee are with the Institute for Infocomm Research, Agency for Science, Technology and Research (A*STAR), Singapore 138632 (e-mail: ctguan@i2r.a-star.edu.sg; kkang@i2r.a-star.edu.sg; kptee@i2r.a-star.edu.sg).

Color versions of one or more of the figures in this paper are available online at http://ieeexplore.ieee.org.

Digital Object Identifier 10.1109/TBME.2013.2248153

very LF band and the high gamma band in premotor, prefrontal, and parietal regions revealed direction-related information. The study reported in [17] used signals from the Posterior Parietal Cortex (PPC) region to decode intended movement direction during a delayed saccade or reach task using Independent Component Analysis (ICA).

In a study using MEG and EEG [14], [15], signals in the LF band (2–5 Hz) were found to contain movement-speed-related information. Another study [19] used event-related spectral perturbation and event-related potential of sensory motor rhythm to analyze speed-related features. The study in [18] reported a possibility of identifying different types of movements and speed using an EEG-based system and the authors performed single trial classification using the rebound rate of Movement-Related Cortical Potentials (MRCP) and power in mu and beta band as features. The reconstruction of hand movement velocities using EEG was discussed in [20] and [21] for 2-D and 3-D movement, respectively. The reported correlations between recorded and reconstructed velocities are highly motivating. A study reported in [22] investigated the relationship between kinematics of imagined and actual hand movement and reported possibility of continuous decoding.

Motivated from these studies, in our current study, an experiment was performed to investigate the presence of movement-related parameters from EEG signals in the LF band. The focus of this study is to classify and reconstruct the speed of movement using LF components of EEG and to study how these are affected if the movement is performed in four different directions. The aim of this research is to develop a BCI with a more refined control or increased number of control commands for movement by including information regarding movement speed.

The challenges in developing an efficient feature extraction algorithm in EEG-based BCI research are to address the issues of low signal-to-noise ratio, nonstationarity, and spatial localization of the discriminative features [1]. To tackle these problems, a Wavelet-Common Spatial Pattern (Wavelet-CSP) algorithm was used. A Wavelet-CSP algorithm using a single decomposition level was used in [23] to reconstruct and denoise the signal before applying common spatial pattern (CSP) for applying in BCI Competition III Dataset I [33]. In [24], a Wavelet-CSP approach was used combined with fuzzy logic in an asynchronous offline BCI system. In this study, the proposed Wavelet-CSP algorithm creates time-frequency-space localized signal by multiple levels of decomposition of signal. A preliminary version of this study was reported in [25] by the authors, to classify directional information from EEG. In this study, the Wavelet-CSP algorithm is used to extract the speed-related features from EEG, and the algorithm has been enhanced to extract the optimal levels of wavelets. The proposed approach in this study decomposes the preprocessed EEG using wavelets and subsequently reconstructs it at different levels to yield subband signals that are further spatially filtered using CSP algorithm. To the best of our knowledge, this approach of Wavelet-CSP algorithm using LF features has not been used to analyze or classify movement-related parameters till date. An experiment was designed based on these requirements and EEG data collected during right-hand movement was used to validate the algorithm. The W-CSP filtered signal was used to: 1) classify the movement parameters; and 2) reconstruct the 2-D speed profile.

The rest of the paper is organized as follows: Section II presents the proposed Wavelet-CSP algorithm. Section III describes the experiment performed and the data analysis steps. Section IV presents the results and discussions, followed by conclusions in Section V.

II. Proposed Feature Extraction Algorithm

In order to extract the features corresponding to speed from LF region of EEG, a feature extraction algorithm that can provide high-resolution decomposition of very LF signals is required. This property is assumed to provide higher performance for classification or reconstruction of movement parameter speed. An orthogonal filter bank-based Wavelet transform (WT) suits this requirement with the added advantage of high-temporal localization. Wavelet analysis [26], [27] is widely used in BCI systems to extract the discriminative features from time-frequency plots. The proposed Wavelet-CSP algorithm incorporates spatial filtering using the CSP algorithm, which is an efficient method to extract the discriminative EEG features. The CSP algorithm has been enhanced with various frequency band optimization techniques such as Filter Bank CSP (FBCSP) [28]. Although FBCSP yielded superior accuracy in classification of right- and left-hand motor imagery (MI) on the BCI Competition IV Dataset II a [33], its fixed frequency resolution and inferior performance in LF bands hinder its use to identify movement-related parameters. Hence, the adopted Wavelet-CSP algorithm uses wavelet-based subband technique instead of filter bank-based subband.

A. Discrete Wavelet Transform (DWT) and Filter Banks

The DWT effectively addresses the tradeoff between time and frequency resolution in nonstationary signal analysis. Wavelets are single prototype functions, similar to a bandpass filter, whose contracted version (high frequency) performs fine temporal analysis and dilated version (LF) performs fine frequency analysis [30]. The WT of a continuous time signal *x(t)* can be defined as

$$X_w\left(a\ \ b\right) = \frac{1}{\sqrt{a}}\int_{-\infty}^{\infty} h^{*}\left(\frac{t-b}{a}\right) x\left(t\right) dt \tag{1}$$

where $a \in R^{+}$, b $\in$ *R,* and $h*(\ )$ represent the conjugate of basis function obtained by the translation and dilation of single prototype wavelet [29].

To remove the redundancy caused by the continuous parameters (*a, b*), discretization is carried out as $a = a_0{}^{\ m}$ and $b = na_0{}^{m} b_0$ $a_0 > 1$, $b_0 \neq 0$, *m, n* $\in Z$. Thus, on the discrete grid, WT is obtained as DWT given by

$$X_w\left(m\ \ n\right) = a_0^{-m\ \ 2}\int_{-\infty}^{\infty} h\left(a_0^{-m}t - nb_0\right) x\left(t\right) dt \tag{2}$$

We use the discretization on dyadic grid, $a_0 = 2$ and $b_0 = 1$ so that the set of functions $h(\ )$ is orthonormal. The dyadic

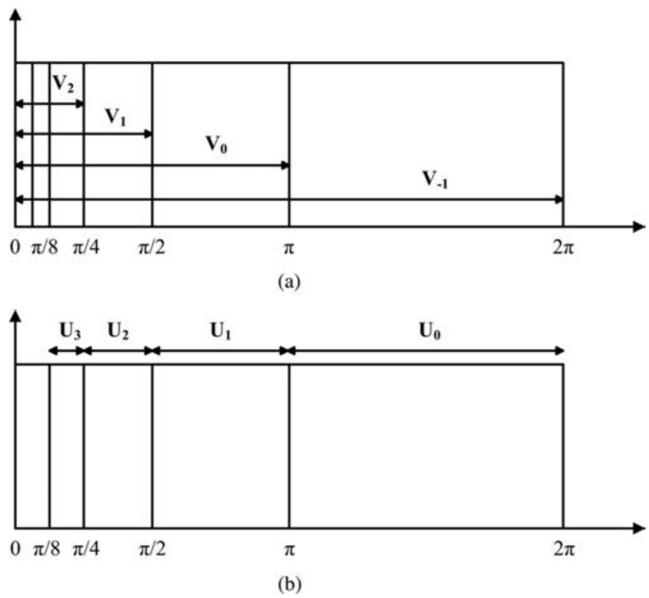

Fig. 1. Ideal spectrum division using DWT.

case of DWT forms an octave band filter, and hence, it can be interpreted as a constant Q-filtering using a set of octave band filters followed by sampling at their respective Nyquist frequencies. Each higher octave band introduces details or higher resolution to the signal. This is the basic concept of multiresolution analysis and is used to construct orthonormal bases of wavelets.

The concepts of multiresolution and successive approximation can be explained as follows. Let V_i for $I \in Z$, be defined as the space of band limited functions with frequencies in the interval $(-2^{-i}\ \pi, 2^{-i}\pi)$ and U_i is the orthogonal complement of V_i in V_{i-1} which spans the frequencies $(-2^{-i+1}\ \pi, -2^{-i}\ \pi)$ U $(2^{-i}\ \pi, 2^{-+1}\ \pi)$. These spaces are related as in the following equation [23]:

$$V_i \subset V_{i-1} \qquad V_{i-1} = V_i \oplus U_i \tag{3}$$

The decomposition of space V_{i-1} into U$_i$ and V_i is essentially a WT on discrete sequences. The orthonormal wavelet bases are constructed such that they span V_i and U_i respectively. For instance, at $i = 0$, the functions that approximate signals of space V_{-1} in V_0 represent a perfect half-band low-pass filter and in U_0 represents a perfect half-band high-pass filter. The ideal division of spectrum discussed previously can be pictorially represented as in Fig. 1. This type of multiresolution analysis using wavelets is used to analyze the signal in our method, so that signal features in different subbands can be separately analyzed.

B. Common Spatial Pattern

The CSP algorithm is often used to optimally discriminate between two classes of EEG data based on simultaneous diagonalization of two covariance matrices [10]. A brief description of CSP is given in this section. Given that, the preprocessed EEG data in a single trial are represented as matrix X of size $N \times T$, where N is the number of channels used and T is the number of samples recorded in each trial from each channel. The CSP projection matrix W is used to obtain the spatially filtered EEG signal as in

$$Z = WX \tag{4}$$

The rows of W are the stationary spatial filters and columns of W^{-1} represent the common spatial patterns.

The normalized spatial covariance matrix of the EEG data is computed as $C = \frac{XX'}{tr(XX)}$, where X' denotes the transpose of matrix X, and $tr\ (\ )$ represents its sum of diagonal elements of two classes 1 and 2. CSP analysis aims to simultaneously diagonalize these matrices by designing W such that it satisfies

$$W^T C_1 W = \lambda_1 \qquad W^T C_2 W = \lambda_2 \tag{5}$$

where λ_1 and $\lambda\ _2$ are diagonal matrices and satisfies

$$\lambda_1 + \lambda_2 = 1 \tag{6}$$

The CSP projection matrix is determined by eigenvalue decomposition approach. Only a small number of signals j can efficiently discriminate the classes when used to train a classifier. The signals Z_p $(p = 1$ to $2j)$ that maximize discrimination are the ones associated with the largest λ_1 and λ_2, which are the first and last j rows of Z. The feature vectors are obtained as in the following equation [10]:

$$f_p = \log\left(\frac{\mathrm{var}\,(Z_p)}{\sum_{i=1}^{2j} \mathrm{var}(Z_i)}\right) \tag{7}$$

The log transformation approximates the normal distribution of data.

C. Wavelet-CSP Algorithm

In this section, we describe the proposed Wavelet-CSP algorithm. The first step is to construct an orthogonal filter bank using wavelets. From a signal processing approach, we can define DWT as applying filters and samplers on square summable discrete time sequences, to perform a coarse half-resolution approximation of the original time sequence [29]. As mentioned in Section II-A, we use orthonormal wavelet bases, which spans V_i and U_i to perform filtering. The wavelet decomposition involves filtering with a half-band low-pass filter and half-band high-pass filter followed by subsampling by 2. The signals can be reconstructed from these subspaces using the reverse process, i.e., up sampling by 2 and filtering using time reversed filter sequences. Fig. 2(a) demonstrates the process where the impulse response of decomposition and reconstruction filters are represented by $h_{0\ \ 1}(n)$ and $h_{0\ \ 1}(n)$, where h_0 provides the lower half-band and h_1 gives higher half-band filters, and h denotes the time reversed h.

The preprocessed EEG in a single trial is represented as $X = [\boldsymbol{x}_1, \boldsymbol{x}_2, \quad , \boldsymbol{x}_N]^T$, where each $\boldsymbol{x}_c$ are T-length sequences given by $\boldsymbol{x}_c = [x_c\ (0)\ \ x_c\ (1) \qquad x_c\ (T-1)]$. The impulse response of filter is in the form of $\boldsymbol{h}_o = [h_o(0)\ \ h_o(1) \qquad h_o(k-1)]$. The assumption is that the even shifted versions of the impulse response, i.e., the rows of H_0 given in (8), as shown at the

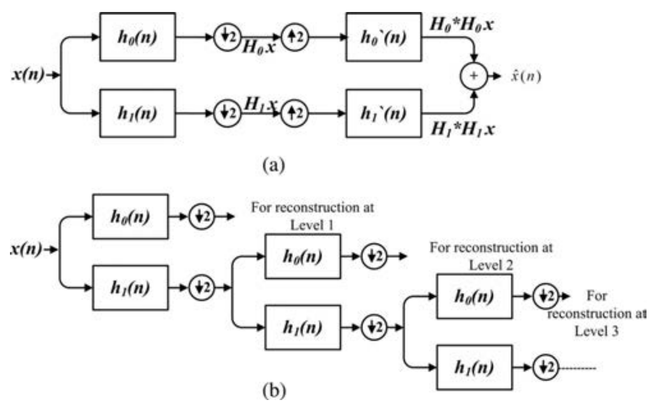

Fig. 2. (a) Signal decomposition and reconstruction using filters and up/down sampling, (b) signal decomposition into subspaces to produce similar results as in DWT at each level.

bottom of the next page, forms an orthonormal set, which spans the subspace V_o

We derive a filter with impulse response as in (9) and its even shifted version such that it spans the subspace U_0 to form H_1

$$h_1(n) = (-1)^n\, h_0(L-1-n) \tag{9}$$

H_1 and H_0 are structurally similar and the orthonormal sets formed by the filter responses and the nonoverlap of the subspaces spanned by them can be notated as

$$H_0 H_0^* = I \;\; H_1 H_1^* = I \;\; H_0 H_1^* = 0 \tag{10}$$

The signal is, thus, projected to subspaces V_0 and U_0 followed by subsampling as P_0 and P_1 by

$$P_0 = H_0 \boldsymbol{x}_c \quad P_1 = H_1 \boldsymbol{x}_c \tag{11}$$

Here, P_0 consists of the detailed coefficients and P_1 consists of approximation coefficients. This is one level of wavelet decomposition. The reconstruction of signal is achieved using the complex conjugates of H_0 and H_1 as in

$$\boldsymbol{x}_c = H_0^* H_0 \boldsymbol{x}_c + H_1^* H_1 \boldsymbol{x}_c \tag{12}$$

The reconstruction in the lower and higher subband is carried out by zero padding the coefficients, P_0 and P_1 and multiplying it with complex conjugates of H_0 and H_1 respectively. Fig. 2(b) shows the multilevel structure, wherein the aforementioned process repeats at each level.

We use Daubechies wavelets for the creating filter banks. In order to decompose very LF with high resolution, we have adopted a scaled to zero decomposition [31] in which the decomposition up to maximum number of levels, given by $L = \log_2 T$, where T is the number of samples in the signal. The detailed coefficients, P_0 at each level is obtained as D_L, D_{L-1}, ,D_1 and the approximation coefficient, P_1 for highest level as A_L. The signals in each subband are obtained by wavelet reconstruction of these wavelet coefficients as X_W^l. The subband signals are spatially filtered using CSP. The W-CSP filtered signal in each of the subbands l ($l = 1$ to $L+1$) is obtained as in

$$Z_W^l = W_l X_W^l \tag{13}$$

The most discriminative features are calculated using (7) in each l and these are used to train a Fisher Linear Discriminant (FLD) classifier which is explained in Section II-D. In a parallel study aiming at reconstructing the movement speed profile, the W-CSP filtered signals are used to train a Multiple Linear Regressor (MLR) model. This is explained in Section II-E. The block diagram illustrating the proposed Wavelet-CSP algorithm along with the analysis performed is shown in Fig. 3 and the steps involved are described as follows.

Step 1: The EEG data are acquired and preprocessed with low pass and notch filtering.

Step 2: The preprocessed signal is projected into subbands by wavelet decomposition.

Step 3: The signals at different subbands are reconstructed using wavelet reconstruction.

Step 4: The subband signals are spatially filtered using CSP.

Step 5: The discriminative features are extracted from W-CSP filtered signal. A FLD classifier is trained using these features and performance of algorithm in terms of classification accuracy is determined.

Step 6: The W-CSP filtered signal is used to reconstruct the speed profile and the decoding accuracy in terms of correlation coefficient is calculated.

D. FLD Classifier

The FLD [28] is a linear discriminant that maximizes the ratio of between class scatter to within class scatter given by

$$J(F) = \frac{F' S_B F}{F' S_W F} \tag{14}$$

where S_B is the between class scatter matrix and S_w is the within class scatter matrix obtained from the feature space.

E. Multiple Linear Regressor

The speed profile is reconstructed using a MLR model, which is a linear fitting strategy over multiple regressor variables. We define two types of reconstruction models using the subband signals obtained from the proposed W-CSP algorithm. Here, s_v represents the recorded speed, where $v\varepsilon \;\; x \;\; y$ absolutespeed The weights a_v^1 a_v^2 $b_{c\tau v}$ and b_{clv} are estimated using through multiple linear regression.

$$H_0 = \begin{bmatrix} \ddots & \vdots & \vdots & & \vdots & \vdots & & \vdots & \ddots \\ & h_0(k-1) & h_0(k-2) & & h_0(1) & h_0(0) & 0 & 0 & \\ & 0 & 0 & h_0(k-1) & & & h_0(1) & h_0(0) & \\ \ddots & \vdots & \vdots & & \vdots & \vdots & & \vdots & \ddots \end{bmatrix} \tag{8}$$

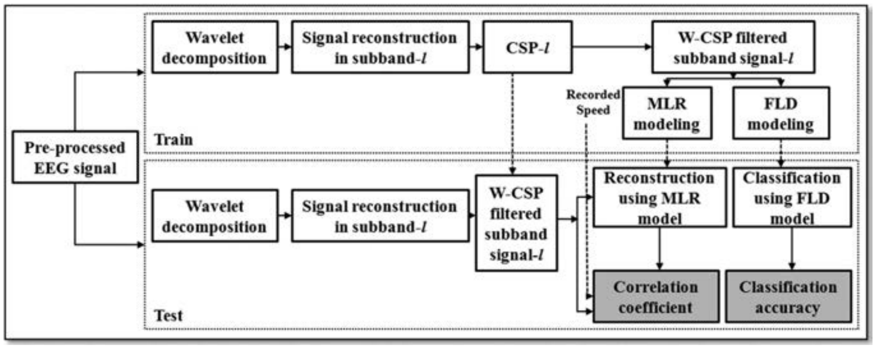

Fig. 3. Proposed wavelet-CSP algorithm.

Model 1: The W-CSP filtered signal in the lowest subband $(L + 1)$ and its time shifted versions are used to construct this model. The number of time-lagged components T_l is set to 5 and each of the components are 10 ms shifted from the previous one

$$s_v^1(n) = a_v^1 + \sum_{c=1}^{N} \sum_{\tau=0}^{T_l} b_{c\tau v} Z_W^{L+1}(n - 5 \quad \tau) \tag{15}$$

Model 2: The W-CSP filtered signal in various subbands l are the constituents of this model.

$$s_v^2(n) = a_v^2 + \sum_{c=1}^{N} \sum_{l=1}^{L+1} b_{clv} Z_W^l(n) \tag{16}$$

Equations (15) and (16) are defined for the x and y components of speed and its absolute value.

III. Experiment

An experiment was performed to collect EEG data while the subjects performed right-hand movement at two different speeds in four different directions. Visual cues were provided to instruct the subjects to perform the task.

A. Subjects and Equipments

The experiment was performed in the Brain Computer Interface Laboratory of Institute for Infocomm Research, Agency for Science, Technology and Research, Singapore. EEG data were recorded from seven subjects while executing the instructed movement. All the subjects are healthy males. The data were recorded at lower cutoff frequency of 0.05 Hz, using Neuroscan SynAmps 128 channel EEG Amplifier with a sampling rate of 250 Hz. The subjects were strapped to the MIT MANUS robot [34] while performing the task to record the exact hand position and speed at every sample time. Data were recorded from 118 channels along the scalp and 35 channels spanning the sensory motor area were used for analysis.

B. Experiment Protocol

The types of hand movements studied were fast and slow movements in four directions: North, South, East, and West.

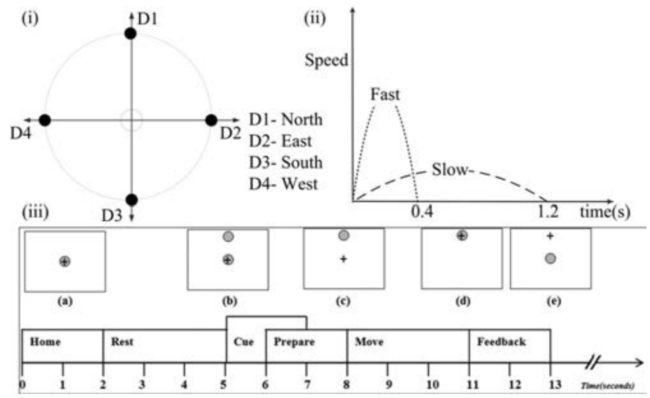

Fig. 4. (i) and (ii) Directions and speeds studied. (iii) Experiment Timeline.

The movements were performed in the horizontal plane. North refers to hand movement outwards and away from the body, South refers to movement inwards and toward the body. East and West refer to movement toward the right and left side, respectively. The slow movement refers to movement that takes more than 1200 ms and fast refers to movement that takes less than 400 ms to perform a movement covering 15 cm in this plane in the specified direction. These details of the experiment protocol are shown in Fig. 4.

The experiment timeline along with the visual display provided is shown in Fig. 4(iii). The subject was seated on a chair with arm resting on a table and facing a computer monitor that provided visual feedback. The subjects were requested to refrain from the eye movements to prevent electrooculographic (EOG) artifacts. The home screen showed an encircled cross as given in part (a) of Fig. 4(iii) and this was shown during the entire rest period. At the end of 4 s of rest, cue was given as shown in part (b) of Fig. 4(iii), which corresponds to North direction. The target location, presented as an empty circle, could be anywhere in the four directions mentioned. This was followed by a preparation time for 2 s, at the end of which the circle around the cross disappeared as in part (c) of Fig. 4(iii). This denoted the onset of movement in which subject was given up to 3 s to complete a movement, at the end of which the cross appeared at the target position part (d) of Fig. 4(iii). If subject fails to reach the correct target within the given time, the trial was flagged and later rejected. The subject was notified this during the following 2 s. A successful trial was indicated by the reappearance of circle as in part (e) of Fig. 4(iii). The display is returned to home screen and this cycle was repeated.

The experiment was conducted in two sessions of 50 cycles each. In each cycle, eight trials were performed by the subject. Each cycle was divided into slow and fast movement sets of four trials each. The task-slow was cued by 11.25-mm diameter target circle and the task-fast was cued by a target circle with a diameter 1.5 times that of target circle for task-slow. Each of these sets comprised of trials in four directions in a randomized order. Each trial took around 13 s to perform and the total recording time for a single subject was approximately 2 h and 45 min.

C. Data Analysis

The preprocessing step of the recorded EEG data included low-pass filtering at 100 Hz and a notch filter at 50 Hz. EOG artifacts were removed using ICA [35] approach, which nullified the signal components that are highly correlated with the recorded EOG. The time segments for analysis were chosen, as the last 1 s of movement preparation and the first 1 s of movement execution. The data preprocessing was followed by the feature extraction, where the proposed Wavelet-CSP algorithm was used to extract the features. The cross-validation analysis splits the dataset into nonoverlapping training and test data. The W-CSP filter was constructed using the training dataset, which is later used to filter the test data. The features obtained from the training dataset was used to train a FLD classifier and the classification performance on the test dataset was measured in terms of mean classification accuracy and standard deviation. The MLR model was also generated using the training data and this is applied to the test data during each fold of cross validation. The following analyses were then performed:

Analysis 1: Much of the researches in this area concentrate on identifying the informative features for speed and direction decoding [15]–[22]. As mentioned in Section I, the work in [17] has analyzed PPC for intended movement using ICA and the method in [18] used rebound rate of MRCP for classifying speed for different experiment paradigms. To the best of our knowledge, no methods available in the literature explored the low frequencies (<7 Hz) of EEG using wavelets. Hence, for a comparative study, we use a CSP algorithm for EEG low pass filtered at 7 Hz and calculate the performance. Next, we rebuilt a FBCSP for very LF EEG data analysis. The performance in three frequency regions, namely low frequency, LF (<7 Hz), high frequency, HF (7–100 Hz), and the entire Band (0–100 Hz) were studied. The resolution of FBCSP in LF and HF bands were 2 and 4 Hz, respectively. The performance of WCSP algorithm at LF, HF, and the entire frequency range were also calculated. For this, the levels corresponding to each of the frequencies were reconstructed. Also the performance of WCSP algorithm using different wavelets and its higher orders were studied. The higher order Symlets and Daubechies were considered.

Analysis 2: As our study dealt with actual hand movement, the data could possibly be affected by electromyography (EMG) due to muscular activation. EMG signals reflect activation of multiple muscles and, hence, activate multiple motor units of brain thereby producing a diffused activity in scalp. Hence, we used a Laplacian spatial filter that accentuates localized activity whereby the diffused activity of EMG is suppressed. Here, a finite difference method reported in [32] is used to the derive Laplacian filter. The filtered signal is obtained using the following equations:

$$X_i^{\mathrm{LAP}} = X_i - \sum_{j\in S_i} g_{ij} X_j \quad g_{ij} = \frac{1\ \ d_{ij}}{\sum_{j\in S_i} 1\ \ d_{ij}} \tag{17}$$

where S_i is the set of electrodes surrounding the ith electrode and d_{ij} is the distance between electrodes i and j (where j is a member of S_i).

Analysis 3: The aim of this study is to analyze features related to speed from EEG data. Hence, in this analysis all trials from a subject were used irrespective of the direction in which they performed hand movement. For illustrating the influence of LF bands and to validate the level selection process, the proposed Wavelet-CSP algorithm was performed using different number of reconstructed subbands. We start with using coefficients from all levels (L), that gives $(L + 1)$ subband signals and then by eliminating contents of one lower level at each time for reconstruction. The objective is to determine the number of levels that can be eliminated without degrading the performance of classifier. In our analysis, if the number of subbands used is L_V, then the coefficients considered for reconstruction are as given in

$$\begin{array}{lll} A_L\ \ D_L\ D_{L-1} & \qquad D_{L-L_v+2} & \quad \text{for } L_V \neq 1 \\ A_L & & \quad \text{for } L_V = 1 \end{array} \tag{18}$$

The performance of algorithm in terms of cross-validation results were calculated for $L_v = 1$ to $L + 1$.

Analysis 4: The applicability of the proposed approach to reconstruct the speed profile is studied in this section. The MLR models proposed were used to reconstruct the absolute, x and y components of speed. The decoding accuracy was measured in terms of Pearson's linear correlation coefficient. The results are compared with the study reported in [21].

Analysis 5: In order to find the physiological significance of the algorithm and the source of the informative features in the brain, we studied the spatial patterns obtained from CSP for movement at each speed.

IV. Results and Discussion

The results followed by inferences of *Analysis 1–5* are given in Sections 1V-A–E.

A. Comparisons

The results of the comparison of various approaches are given in Table I. Various conclusions are drawn from the results. The results using a simple low-pass filtering at 10 Hz followed by CSP [10] is considered as the baseline result (mean accuracy of 62.83%). Further comparing FBCSP [28] and Wavelet-CSP, we can see that Wavelet-CSP outperforms FBCSP in all the

TABLE I
PERFORMANCE OF SPEED CLASSIFICATION FOR VARIOUS METHODS

Subject v/s Method	W-CSP (sym5)			CSP	FBCSP			Different types of wavelets					
	Low Freq.	High Freq.	All freq.	Low Freq	Low Freq.	High Freq.	All freq.	db1	db2	db3	db4	db5	sym4
1	**89.17**	61.83	85.73	63.44	92.55	68.40	73.74	89.79	87.07	93.75	94.17	92.18	93.44
2	**91.98**	61.45	89.06	56.25	72.09	50.74	65.20	86.45	91.14	90.29	91.36	91.45	91.13
3	**88.23**	64.69	81.46	67.47	78.38	79.61	71.88	82.91	87.49	83.55	84.27	85.32	84.58
4	**79.28**	69.80	78.55	67.29	65.00	61.26	61.95	77.08	78.22	81.15	81.04	80.32	82.82
5	**68.01**	63.54	70.29	60.64	68.31	49.74	62.71	71.98	67.28	64.39	70.83	70.71	68.02
6	**91.67**	61.04	87.49	66.98	85.89	58.39	82.06	81.55	89.36	87.81	87.92	88.64	89.06
7	**77.63**	57.12	76.19	57.71	53.73	56.25	51.43	72.96	76.20	79.52	72.86	75.00	76.29
Mean	**83.71**	62.79	81.25	62.83	73.71	60.63	66.99	80.39	82.40	82.92	83.21	83.37	83.62

TABLE II
PERFORMANCE OF SPEED CLASSIFICATION USING 3×3 CROSS VALIDATION (MEAN CLASSIFICATION ACCURACY IN PERCENTAGE)

Subject	*Proposed W-CSP algorithm	Incorporating Laplacian spatial filtering	Including additional temporal and occipital electrodes
1	89.17	89.49	92.18
2	91.98	89.37	96.14
3	88.23	89.06	89.16
4	79.28	81.26	73.64
5	68.01	68.54	87.28
6	91.67	90.63	88.43
7	77.63	74.88	80.59
Mean	83.71	83.32	86.77
*p-value	-	0.5843	0.3491

**p*-value indicates paired t-test results.

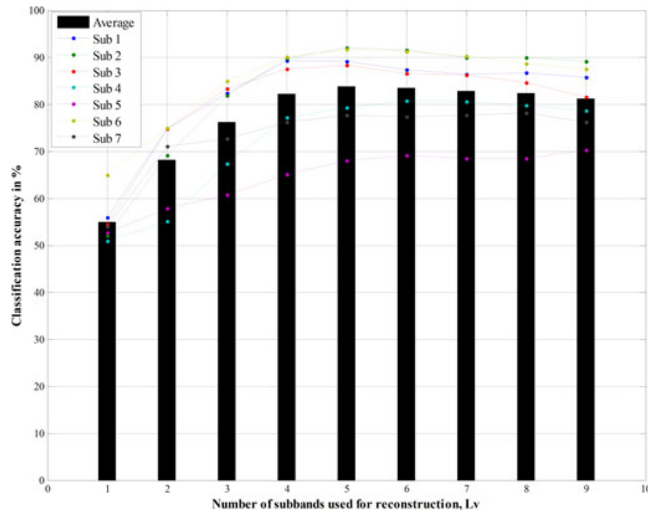

Fig. 5. Effect of using different number of subbands for classification. The results are for speed classification (fast versus slow movement).

frequency bands. The results provide two important conclusions. First, in both algorithms, the lower frequencies seem to perform better than others. This agrees with the results reported in various studies [13], [15], [16] and in the review articles [12], [14], that the LF band contains movement parameter information. Second, the poor performance of FBCSP can be accounted by its lack of time localization which is provided by Wavelet-CSP. Also the filter bank design at low frequencies is hard to achieve.

The performance of algorithm using various wavelets is also shown. It is found to increase at higher orders and Symlets wavelet of order 5 (sym5) performed the best in our algorithm giving an accuracy of 83.71%. However, on increasing the order further, the performance in terms of accuracy is found to decrease. For the further analyses, we have used the best performing "sym5" wavelet.

B. Effect of Muscular Activation

The results of the approach adopted to remove EMG contamination is given in Table II. Column 1 indicates the performance using the proposed W-CSP algorithm and mean accuracy for classifying speed is obtained as 83.71%. Column 2 shows the performance using Laplacian filtering for EMG removal gives almost similar performance of accuracy 85.04%. Also, the results from these two approaches showed no statistical significance ($p = 0$ 5843). The identical performance points out that the EMG, if present, does not provide any discriminative information about movement kinematics. The results in column 3 of Table II uses the W-CSP approach including additional electrodes from the temporal and occipital electrodes. The results obtained prove that inclusion of more electrodes does not change the performance significantly ($p = 0$ 3491).

TABLE III
CORRELATION COEFFICIENT BETWEEN RECONSTRUCTED AND RECORDED SPEEDS

Subject	Ref. [21]			Proposed Method (1) in eq. (14)			Proposed Method (2) in eq. (15)		
	x	*y*	*Abs.*	*x*	*y*	*Abs.*	*x*	*y*	*Abs.*
1	0.30	0.23	0.34	0.59	0.41	0.56	0.56	0.44	0.49
2	0.21	0.05	0.21	0.41	0.22	0.46	0.52	0.43	0.49
3	0.23	0.14	0.35	0.49	0.19	0.61	0.50	0.30	0.58
4	0.25	0.19	0.21	0.59	0.28	0.35	0.66	0.49	0.46
5	0.14	0.03	0.42	0.36	0.22	0.49	0.36	0.31	0.36
6	0.25	0.23	0.37	0.41	0.47	0.58	0.50	0.57	0.58
7	0.19	0.15	0.33	0.28	0.37	0.56	0.29	0.39	0.55
Mean	*0.22*	*0.15*	*0.32*	***0.45***	***0.31***	***0.52***	***0.48***	***0.42***	***0.50***

Ref. [21] : Results obtained by applying the method mentioned in [21] to our data.

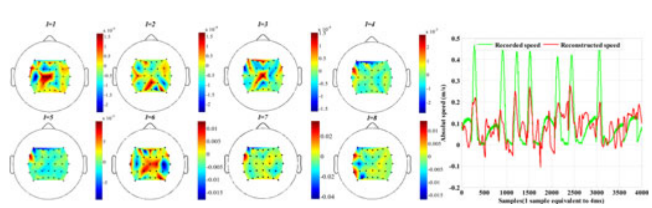

Fig. 6. MLR coefficients for eight subbands used, and the recorded and reconstructed speed profiles.

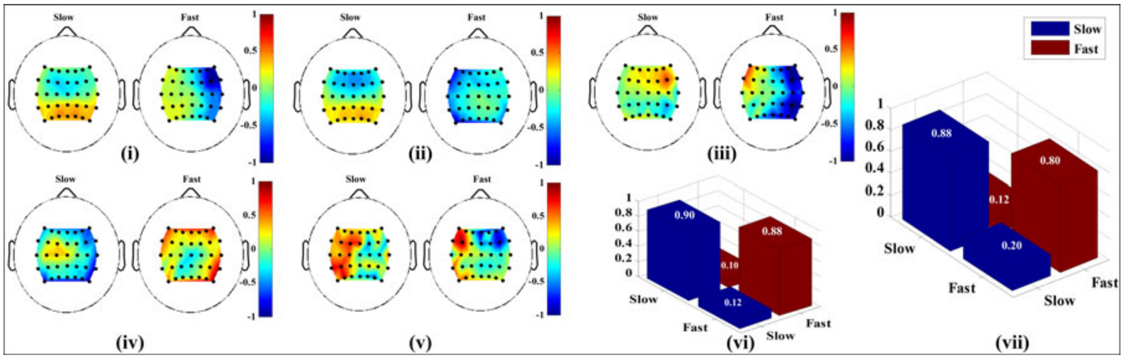

Fig. 7. (i)–(v) Spatial patterns obtained at five lower frequency subbands by W-CSP method for subject 1, (vi) confusion matrix for subject 1, and (vii) average confusion matrix for seven subjects.

C. Classifying Speed of Movement

The mean classification accuracy and variance were calculated for each of the seven subjects by 3×3 fold cross validation. In order to study the levels of wavelet decomposition containing optimal information, the classification was performed for $L_V = 1$ to $L + 1$. The results obtained are shown in Fig. 5. From the graph, it is seen that for $L_V = 5$, the maximum accuracy of (83.71 8.98)% is obtained. The accuracy decreases for levels, $L_V > 5$. Hence, we have used only five informative levels for our further analysis. The literature [11]–[14] which clearly mentions the presence of kinematic information in the very LF band (<7 Hz). For $L_V = 5$, the chosen subbands represent this LF subband of EEG signal. According to (3) and (18), $L_V = 5$ is found to correspond the frequency range 0.05–6.25 Hz. Hence, the results obtained affirm the findings of various works.

D. Reconstructing Speed of Movement

Table III shows the Pearson's linear correlation coefficient values obtained between recorded speed and reconstructed speed as mentioned in methods 1 and 2 of Section II-E. [21] reported reconstruction of 3-D movement kinematics using MLR approach. This method is applied on our 2-D data and the results obtained are summarized in the table. Comparing the two proposed approaches, the x and y components of speed are better reconstructed by the proposed method 2, whereas the absolute speed profile is better decoded by the proposed method 1. The significant correlation values obtained in the proposed methods prove that W-CSP filtered signals can efficiently be applied for the reconstruction of movement speed. Fig. 6 shows the reconstructed and recorded speed profile for subject 1 and these display high correlation with each other. This profile consists of both slow and fast movements from the test data of cross validation. Fig. 6 also shows the spatial distribution of MLR coefficients from Model 2, given by (16) in each of the subbands and it demonstrates the involvement of parietal and contra lateral motor areas in almost all subbands. It should also be noted that the coefficient values are higher in the LF subbands ($l = 6$ to 8) compared to the rest.

E. Discriminating Features as Shown by CSP

The analysis results of spatial pattern is provided in this section. Fig. 7(i)–(v) shows the W-CSP plots obtained for speed classification. In the plot, the channels taken for analysis are shown as black dots. The spatial patterns for subject 1 obtained from the ($L_v = 5$) levels used are shown. The confusion matrix averaged over all cross-validation folds for subject 1 is given in Fig 7(vi). The mean confusion matrix over all subjects is given in Fig. 7(vii). The high and nonbiased performance of the technique is indicated by the leading diagonal bars in the plot. From the spatial plots, it is evident that the discriminative brain activity is seen mostly in the parietal and left motor cortex region. The planning and estimation of movement kinematics is performed by PPC of the brain as mentioned in [17]. Also the right-hand movement results in an activation in the contra lateral hemisphere that in this case is the left side of the cortex.

This study utilizes the features extracted from LF EEG using the Wavelet-CSP technique proposed to classify and reconstruct hand movement speed. The LF (<6.25 Hz) EEG performs better in classifying movement speed information and the spatial distributions obtained shows involvement of contra lateral motor as well as parietal cortex. Our findings is in line with various results in literature [12]–[22] using EEG, ECoG, and MEG. The results obtained justify the application of W-CSP technique for finer movement control in terms of speed, in an EEG-based BCI system by efficiently identifying the underlying neural activity.

Furthermore, any movement is associated with a change in more than one of its parameters. In this study, the movement task involves variation in movement force along with speed. Being a coexisting factor of movement speed, the EEG data collected are likely to be influenced also by changes in movement force. However, identifying the contributions of force and speed to EEG separately is beyond the scope of this study. In our future work, we intend to design experiments that can provide resolved information on various movement parameters such as force, direction, extent, etc.

V. Conclusion

The objective of this study was to design an algorithm that can extract the information regarding movement-related parameter:

speed. The LF bands of movement-related potentials recorded by EEG were exploited using a highly time-frequency-space localized algorithm in order to extract features relevant to speed. A Wavelet-CSP algorithm has been proposed, which effectively localizes signal in time, frequency, and space and provides discriminative features for classifying speed. To the best of our knowledge, such an approach using LF features to classify speed of movement was not adopted in literature to date. The filtered signals are also applied to reconstruct the speed profile. The algorithm was validated using EEG data collected during an experiment, where the subject executed right-hand movement in two different speeds in four different directions. It was confirmed that the performance of the algorithm was not influenced by EMG by using Laplacian filtering. The results obtained showed that the parameter, speed, can indeed be classified and reconstructed from EEG signal during an actual movement. The algorithm was further analyzed and the conclusions obtained were discussed in the previous section. A mean classification accuracy of 83.71% was obtained for the speed of movement at an optimal chosen number of subbands. The performance for speed classification in different directions was also studied. A linear correlation of 0.52 was obtained between the recorded and reconstructed speed. The spatial patterns showed the activation in contra lateral motor area and parietal regions.

The motivation behind BCI research is its applicability in MI. This study also hopes to be further extended to analyze MI signals. The features related to movement parameters must have a major overlap in both actual movement and MI. The future work also includes exploring the MI signals to analyze other movement parameters such as extent of movement. The results of our proposed algorithm showed the possibility of introducing a refined control command set to BCI system by identifying the features related to movement parameters. The high performance of our algorithm and the relevance of this approach can be further explored to build an efficient BCI system.

REFERENCES

[1] G. Dornhege, J. R. Milan, T. Hinterberger, D. J. McFarland, and K.-R. Muller, *Towards Brain- Computer Interfacing*. Cambridge, MA, USA: MIT Press, 2007, ch. 1.

[2] J. R. Wolpaw, N. Birbaumer, D. J. McFarland, G. Pfurtscheller, and T. M. Vaughan, "Brain-computer interfaces for communication and control," *Clin. Neurophysiol.*, vol. 113, no. 6, pp. 767–791, Jun. 2002.

[3] G. E. Fabiani, D. J. McFarland, J. R. Wolpaw, and G. Pfurtscheller, "Conversion of EEG activity into cursor movement by a Brain-computer interface (BCI)," *IEEE Trans. Neural Syst. Rehabilitation Eng.*, vol. 12, pp. 331–338, Sep. 2004.

[4] E. Niredermeyer and F. Lopes da Silva, *Electroencephalography: Basic Principles, Clinical Applications and Related Fields,* 5th ed., Baltimore, MD, USA: Lippincott Williams Wilkins, 2004.

[5] G. Pfurtscheller, C. Neuper, D. Flotzinger, and M. Pregenzer, "EEG based discrimination between imagination of right and left hand movement," *Electroencephalography Clin. Neurophysiol.*, vol. 103, pp. 642–651, Dec. 1997.

[6] V. Carmen, N. Kramer, B. Blankertz, and A. Schlogl, "Time domain parameters as a feature for EEG-based Brain-Computer Interface," *Neural Netw.*, vol. 22, pp. 1313–1319, Jul. 2009.

[7] T. Wang, J. Deng, and B. He, "Classifying EEG-based motor imagery tasks by means of time-frequency synthesized spatial patterns," *Clin. Neurophysiol.*, vol. 115, pp. 1–7, Jan. 2004.

[8] A. Schlogl, D. Flotzinger, and G. Pfurtscheller, "Adaptive autoregressive modelling used for single-trial EEG classification," *Biomedical Eng.*, vol. 42, pp. 386–394, Jun. 1997.

[9] J. Muller Gerking, G. Pfurtscheller, and H. Flyvbjerg, "Designing optimal spatial filters for single-trial EEG classification in a movement task," *Electroencephalography Clin. Neurophysiol.*, vol. 110, no. 5, pp. 787–798, May 1999.

[10] H. Ramoser, J. Muller Gerking, and G. Pfurtscheller, "Optimal spatial filtering of single trial EEG during imagined hand movement," *IEEE Trans. Rehabilitation Eng.*, vol. 8, no. 4, pp. 441–446, Dec. 2000.

[11] V. Kaiser, A. Kreilinger, G. R. Muller-Putz, and C. Neuper, "First steps toward a motor imagery based stroke BCI: New strategy to set up a classifier," *Frontiers Neurosci.*, vol. 5, pp. 1–10, Jul. 2011.

[12] S. Waldert, T. Pistohl, C. Braun, T. Ball, and A. Aertsen, "A review on directional information in neural signals for brain-machine interfaces," *J. Physiol.- Paris*, vol. 103, pp. 244–254, Aug. 2009.

[13] T. Ball, A. S-Bonhage, A. Aertsen, and C. Mehring, "Differential representation of arm movement direction in relation to cortical anatomy and function," *J. Neural Eng.*, vol. 6, no. 1, pp. 68–73, Jan. 2009.

[14] K. Jerbi, J. R. Vidal, J. Mattout, F. Lecaignard, T. Ossandon, C. M. Hamame, S. S. Dalal, R. Bouet, and J.-P. Lachaux, "Inferring hand movement kinematics from MEG, EEG and intracranial EEG: From brain-machine interfaces to motor rehabilitation," *IRBM*, vol. 32, pp. 8–18, Feb. 2011.

[15] K. Jerbi, J. P. Lachaux, K. N'Diaye, D. Pantazis, R. M. Leahy, L. Garnero, and S. Baillet, "Coherent neural representation of hand speed in humans revealed by MEG imaging," *Proc. Nat. Academy Sci. USA*, vol. 104, no. 18, pp. 7676–7681, May 2007.

[16] S. Waldert, H. Preissl, E. Demandt, C. Braun, N. Birbaumer, A. Aertsen, and C. Mehring, "Hand movement direction decoded from MEG and EEG," *The J. Neurosci.*, vol. 28, no. 4, pp. 1000–1008, Jan. 2008.

[17] Y. Wang and S. Makieg, "Predicting intended movement direction using EEG from human posterior parietal cortex," in *Proc. 5th Int. Conf. Found. Augmented Cognition. Neuroergonomics Oper. Neurosci.*, Jul. vol. 5638, 2009, pp. 437–446.

[18] Y. Gu, K. Dremstup, and D. Farina, "Single-trial discrimination of type and speed of wrist movements from EEG recordings," *Clin. Neurophysiol.*, vol. 120, pp. 1596–1600, Jan. 2009.

[19] Y. Fu, B. Xu, L. Pei, and H. Li, "Event-related perturbation in spectral power and in potentials during periodic fast and slow motor imagination for brain-controled robots interface," in *Proc. IEEE Int. Conf. Robotics Biomimetics*, Tianjin, China, Dec. 2010, pp. 1299–1304.

[20] J. Lv and Y. Li, "Decoding hand movement velocities from EEG signals during a continuous drawing task," in *Proc. 7th Int. Conf. Fuzzy Syst. Knowledge Discovery*, Yantai, Shandong, China, Aug. 2010, pp. 2186–2189.

[21] T. J. Bradberry, R. J. Gentili, and J. L. Contreras-Vidal, "Reconstructing three-dimensional hand movements from noninvasive electroencephalographic signals," *J. Neurosci.*, vol. 30, no. 9, pp. 3432–3437, Mar. 2010.

[22] H. Yuan, C. Perdoni, and B. He, "Relationship between speed and EEG activity during imagined and executed hand movements," *J. Neural Eng.*, vol. 7, no. 2 (026001), pp. 1–20, Apr. 2010.

[23] L. Zhang, G. Liu, and Y. Wu, "Wavelet and common spatial pattern for EEG signal feature extraction and classification," in *Proc. Int. Conf. Comput., Mechatron., Control Electron. Eng.*, vol. 6, ChangChun, China, Aug. 2010, pp. 243–246.

[24] E. A. Mausavi, J. J. Maller, P. B. Fitzgerald, and B. J. Lithgow, "Wavelet common spatial pattern in asynchronous offline brain computer interfaces," *Biomed. Signal Process. Control*, vol. 6, pp. 121–128, April 2011.

[25] N. Robinson, A. P. Vinod, C. Guan, K. K. Ang, and K. P. Tee, "A Wavelet-CSP method to classify hand movement directions in EEG based BCI system," in *Proc. 8th Int. Conf. Inf., Commun. Signal Processing*, Singapore, Dec. 2011, pp. 1–5.

[26] Y. B. Hua, Y. G. Zheng, Y. R. Guo, and W. Ting, "Adaptive subject based feature extraction in brain-computer interfaces using wavelet packet best basis decomposition," *Med. Eng. Phys.*, vol. 29, pp. 48–53, Mar. 2007.

[27] L. Qin and B. He, "A wavelet- based time-frequency analysis approach for classification of motor imagery for brain computer interface applications," *J. Neural Eng.*, vol. 2, pp. 65–72, Aug. 2005.

[28] K. K. Ang, Z. Y. Chin, H. Zhang, and C. Guan, "Filter bank common spatial pattern (FBCSP) in brain-computer interface," in *Proc. IEEE Int. Joint Conf. Neural Netw.*, Orlando, FL, USA, Jun. 2008, pp. 2390–2397.

[29] M. Vetterli and C. Herley, "Wavelets and filter banks: Theory and design," *IEEE Trans. Signal Process.*, vol. 40, no. 9, pp. 2207–2232, Sep. 1992.

[30] S. Mallat, *A Wavelet Tour of Signal Processing*, 2nd ed. San Francisco, CA, USA: Academic Press, 1999.

[31] H. Zhang, T. B. Ho, M. S. Lin, and X. Liang, “Feature extraction for time series classification using discriminating wavelet coefficients,” in *Proc. Int. Conf. Advances in Neural Netw.*, May 2006, vol. 3971, pp. 1394–1399.

[32] D. J. McFarland, L. M. McCane, S. V. David, and J. R. Wolfpaw, “Spatial filter selection for EEG-based communication,” *Electroencephalography Clin. Neurophysiol.*, vol. 103, pp. 386–394, Sep. 1997.

[33] The BCI competition datasets. (2004). [Online]. Available: http://www.bbci.de/competition/

[34] H. I. Krebs, N. Hogan, M. L. Aisen, and B. T. Volpe, “Robot-aided neurorehabilitation,” *IEEE Trans. Rehabilitation Eng.*, vol. 6, no. 1, pp. 75–87, Mar. 1998.

[35] T. P. Jung, S. Makeig, C. Humphries, T. W. Lee, M. J. McKeown, V. Iragui, and T. J. Sejnowski, “Removing electroencephalographic artifacts by blind source separation,” *Psychophysiology*, vol. 37, pp. 163–178, Mar. 2000.

Neethu Robinson received the B.Tech. degree in electronics and communication engineering from the University of Kerala, India in 2010.

Since August 2010, she has been pursuing the Ph.D. degree from Nanyang Technological University, Singapore. Between January 2012 to March 2012, she was working as Visiting Researcher with the research team of Institute of Medical Psychology and Clinical Neurobiology, University of Tuebingen, Germany. Her major research interests include digital signal processing, multimodal brain computer interfaces, pattern recognition and machine learning.

A. P. Vinod (SM’07) received the B.Tech. degree in instrumentation and control engineering from the University of Calicut, India, in 1994 and the M.Eng. and Ph.D. degrees in computer engineering from Nanyang Technological University (NTU), Singapore, in 2000 and 2004, respectively.

He has spent the first five years of his career in industry as an automation engineer with Kirloskar, Bangalore, India; Tata Honeywell, Pune, India; and Shell Singapore. From September 2000 to September 2002, he was a lecturer with the School of Electrical and Electronic Engineering, Singapore Polytechnic, Singapore. He was a lecturer with the School of Computer Engineering, NTU, from September 2002 to November 2004, and since December 2004, he has been an Assistant Professor with NTU. His research interests include digital signal processing (DSP), low-power and reconfigurable DSP circuits, software radio, cognitive radio, and brain-computer interface. He has published over 150 papers in refereed international journals and conferences.

Kai Keng Ang received the B.A.S.c. (First Hons.), M.Phil. and Ph.D. degrees in computer engineering from Nanyang Technological University, Singapore, in 1997, 1999, and 2008, respectively.

From 1999 to 2003, he was a Senior Software Engineer with Delphi Automotive Systems Singapore Pvt. Ltd. focusing on embedded software for automotive engine controllers. He is now a Senior Research Fellow focusing on brain-computer interface in the Institute for Infocomm Research, Agency for Science, Technology and Research (A*STAR), Singapore. His current research interests include computational intelligence, machine learning, pattern recognition, and signal processing.

Keng Peng Tee received the B.Eng. and M.Eng. degrees in Mechanical Engineering, and the Ph.D. degree in Electrical and Computer Engineering, in 2001, 2003 and 2008, respectively, all from the National University of Singapore.

Since 2008, he has been a researcher at the Institute for Infocomm Research, Agency for Science, Research and Technology, Singapore (A*STAR). His current research interests include control of adaptive and constrained systems, control applications in robotics, and human-robot interactions.

Cuntai Guan (SM’03) received the Ph.D. degree in electrical and electronic engineering from Southeast University in 1993. He is currently a Principal Scientist and Department Head at the Institute for Infocomm Research, Agency for Science, Technology and Research (A*STAR), Singapore.

His current research interests include neural and biomedical signal processing; neural and cognitive process and its clinical application; brain-computer interface algorithms, systems and its applications. He was the recipient of several awards including g.tec Annual BCI Research Award 2010, IES Prestigious Engineering Achievement Award 2009, etc. He has published over 160 refereed journal and conference papers and holds 13 granted patents and applications. He delivered over 30 keynote and invited talks. He serves in the editorial board of IEEE Access, IEEE Transactions on Biomedical Engineering, and Frontiers in Neuroprosthetics. He is a senior member of IEEE.